ELECTRON-BEAM-CHARGED DIELECTRICS— INTERNAL CHARGE DISTRIBUTION*

Brian L. Beers and V. W. Pine
Beers Associates, Inc.

SUMMARY

An electron transport model of the charging of dielectrics due to electron bombardment has previously been given.[1] In this paper, we present a comparison of theoretical calculations based upon this model to measurements of internal charge distributions which have previously been performed.[3] The emphasis is on the distribution of Teflon. Several interesting features of the results are noted. First, the position of the charge centroid as a function of time is not monotonic. Instead, it first moves deeper into the material and then moves back near to the surface. Second, in most time regimes of interest, the charge distribution is not unimodal, but instead has two peaks. Third, the location of the centroid near saturation is a function of the incident current density as has previously been measured.[11] While the qualitative comparison of theory and experiment are reasonable, quantitative comparison shows discrepancies of as much as a factor of two.

I. INTRODUCTION

In the 1978 meeting of this conference two papers[1,2] were presented which provided models for the charging of dielectrics by electron sources. These models included a description of processes occurring internal to the dielectric, and thus permitted the computation of internal charge densities and electric fields. In particular, several computations for internal charge distributions and fields were presented in Reference 1 for the conditions which have become common in laboratory spacecraft dielectric irradiations, monoenergetic kilovolt electrons incident on a free floating dielectric surface. No comparison between the computations and experimental data was presented at that time.

It is the purpose of this paper to compare computations of the internal charge distribution with experimental data for the same quantity which has been reported in the literature.[3] The irradiation conditions correspond to

---

*Supported in part by United States Air Force Space Division under subcontract to SRI, International.

those discussed above. It should also be noted that Frederickson is providing a comparison of other quantities for a metallized front surface in another presentation at this conference.[4] This information, together with two recently published discussions[5,6] of the same subject, will provide a reasonably complete picture of the state-of-the-art of the understanding of this important subject. It is anticipated that the reader will come to the conclusion that a great deal remains to be learned as quantitative agreement is not particularly good.

As noted in Reference 1, for conditions in which the mean electron range is small compared to the dielectric thickness, the external charging characteristics (surface voltage) are effectively decoupled from the details of the internal charge rearrangement in the material. Because these conditions almost universally prevail for the environments of interest (if the Van Allen electrons are ignored), it might be asked why the spacecraft community should care about the fine details represented in these models. Implicit in this question is the assumption that the only parameter of importance is the surface differential potential relative to spacecraft ground. In a presentation by Stevens[7] at this conference, a very strong case is developed which suggests that this is not the case for orbiting spacecraft. In particular, transient pulses associated with breakdown appear to be occurring even when differential voltages are substantially below those required in the laboratory to induce breakdown. The conclusion is that the differential voltage is not the only diagnostic required to understand discharges which occur in space — other more subtle processes may be involved. It was pointed out in Reference 1 that substantial electric fields can exist inside the dielectric even when the external differential voltage is small. This observation provides one speculation about the source of low voltage breakdowns. It is also not difficult to imagine theories of breakdown which depend on a critical trapped charge density.[8,9] Thus, the study of internal charge distributions and fields is probably not some esoteric backwash in spacecraft research, but is rather an essential ingredient in developing an understanding of discharges in space. It is the intent of this paper to provide sufficient data to assess how well this important subject is understood. Conditions in the laboratory are investigated exclusively. The implication for the exoatmospheric environment are left for future investigations.

In Section II, a technical modification to the model is discussed. The modification permits the incorporation of the delayed conductivity in the model. Section III presents the major results of the paper. A discussion of these results is given in Section IV.

II. DELAYED CONDUCTIVITY MODEL

When a free-floating front surface of a dielectric is irradiated with electrons, it is raised to a negative potential relative to the system ground. Electrons arriving later at the sample surface are retarded and consequently penetrate less deeply into the material. This range shortening results in regions of dielectric which are intially irradiated becoming non-irradiated.

Within the numerics of a code model of the process, this leads to regions of dielectric which go from being rather strongly conducting because of the radiation-induced conductivity to the weakly conducting state associated with the dark dielectric. This transition can occur rather abruptly in a Monte Carlo simulation and is distinctly non-physical. This situation can be ameliorated by using improved numerical techniques or by adequately modeling the decay of the conductivity in these regions. We choose the later approach here. The specifics of the approach have previously been given by other researchers.[10]

When dielectrics are subjected to ionizing radiation, charge carriers are liberated giving rise to a radiation-induced conductivity. Since the carriers do not instantaneously recombine when the ionizing radiation ceases, there persists a delayed component of the radiation-induced conductivity. The decay of the delayed conductivity is given by:

$$\sigma = \frac{\sigma'}{1 + bt} \tag{1}$$

where:

σ' = σ_0/F;

σ_0 = conductivity at the end of irradiation;

F = factor by which the conductivity drops in a short (μsec) time ≈3;

t = time in sec; and

b = parameter of order unity.

The above model has been incorporated into the code in the following manner. At each grid point in the dielectric, the newly calculated prompt conductivity, σ_p, is compared to σ' if $\sigma_p < \sigma'$, then the conductivity is obtained from 1), otherwise, the conductivity is set to σ_p.

III. INTERNAL CHARGE DISTRIBUTION

Researchers at Bell Laboratories have developed significant experimental techniques for investigating various features of the internal charge distribution in dielectrics.[3,10,11] These techniques rely inherently on the interpretation of measurements made using electron beam irradiations (so-called split Faraday cup techiques). While other techniques which do not rely on beams have been reported in the literature,[12] to our knowledge these techniques have not been applied to beam charged dielectrics. In this paper, we will rely exclusively on the results of these researchers for providing comparisons.

The material used in all the reported experiments has been FEP Teflon. For the purposes of the primary electron transport, Teflon may be treated as a uniform material with an atomic composition of CF_2 and a density of 2.2 gm/cm^3. Several of the features of the primary transport have already

been published,[1] and will not be reproduced here. It may be recalled that the primary electrons deposit in a region rather broadly distributed about the mean, and that the computational algorithm provides the charge deposition profile Y(x) and the energy dose deposition profile D(x) as a function of the penetration x. The backscatter yield is automatically computed as part of the primary transport. The secondary yield is taken to be proportional to the surface dose in accordance with the model of Burke, Wall, and Frederickson[13] appropriately normalized to fit the monoenergetic data.[14]

The bulk conductivity in Teflon was taken from the data of Adamo, Nanevicz, and Grier.[15] The model assumes that the prompt conductivity is proportional to the local dose rate in the material. The relaxation of this enhanced conductivity to the ambient was discussed in Section II above. The prompt conductivity coefficient K_p is normally taken to have a value of 5×10^{-15} mho/m/rad/sec[14], although this parameter has been varied in some of the calculations reported herein. The value chosen for a particular calculation is indicated with the computed results.

The easiest quantity to obtain experimentally using a split Faraday cup arrangement is the charge centroid $\langle x \rangle$ which is defined by:

$$\langle x \rangle = \frac{\int_0^d x\rho(x)dx}{\int_0^d \rho(x)} \qquad (2)$$

where d is the sample thickness, and $\rho(x)$ is the charge density. The quantity $\langle x \rangle$ represents the mean location of the excess charge in the medium. This quantity has been measured for a variety of charging conditions.[11]

Shown in Figure 1 is a computation of the location of the centroid of charge $\langle x \rangle$ as a function of time. The charging conditions are for normally incident monoenergetic electrons of energy 20 keV at a current density of 3.3 nA/cm^2 incident on a 1 mil sample of Teflon. The transient conductivity coefficient K_p was taken to be 5×10^{-15} mho/m/rad/sec.[13] The addition of the delayed conductivity does not make a significant difference in the temporal behavior of this quantity. Note, in particular, that this quantity initially increases as the deposited electrons are redistributed to the end of the transient conductivity region by conduction processes, and then begins to decrease in longer times as the external potential builds up and slows down the incident electrons. Qualitatively, both models (with and without delayed conductivity) give rise to this same phenomenon. Only the quantitative features are changed by the model change. In any case, the addition of the delayed conductivity more nearly represents the true physics, and is included in all other calculations reported herein.

Shown in Figure 2 is a reproduction of Figure 3 of Reference 11 showing measured values of the charge centroid in Teflon. The charging conditions are for normally incident electrons of varying energies at a current density of

3.3 nA/cm^2 incident on 1 mil Teflon. Three values of <x> are reported, one very near the beginning of the charging, one at the end of the charging time (∿15 sec), and one five minutes after the beam has been turned off. It is clear that the delayed conductivity model is extremely important in modeling this final measurement. Shown in Figure 3 are the time histories of two simulations of the charging conditions of Figure 2 for a 20 keV beam. The two simulations correspond to two choices of the value of the prompt conductivity coefficient K_p. Note that the larger value of K_p gives rise to a more rapid increase in <x> as expected. Generally, the larger value of K_p gives results which are more nearly consistent with the data. The best computed values of <x> at the measured times are indicated on Figure 2. Generally, the computations have the correct qualitative behavior compared to the data (see also Figure 4 of Reference 11), but the computed results show a uniformly smaller penetration. This difference is not understood.

Shown in Figure 4 are the computed time histories of the location of charge centroid for a variety of conditions corresponding to normal laboratory charging operation. Note that the lower energy beams have uniformly smaller value of <x>. Shown in Figure 5 is a scatter plot of the computed values of <x> near saturation for a variety of charging conditions.

An examination of the plots of Figures 4 and 5 indicates that the computed charge centroid location is roughly independent of the incident current density and depends only on the total charge deposited.

This behavior is not in agreement with reported results. As explained in Reference 1 the prompt conductivity is normally taken to be proportional to some power of the local dose rate. The model reported here uses an exponent smaller than unity, the computational results become strongly dependent on the value of the incident current density. Shown in Figure 6 is a reproduction of Figure 6 of Reference 11, which presents data on the dependence of <x> versus beam current density. The decrease in <x> for larger values of the current density strongly suggests a nonlinear dependence of the prompt conductivity on dose rate. The present model can adequately represent this behavior. Because sufficient independent data on this nonlinearity does not appear to be available, no attempt was made to generally incorporate this behavior in the model. Reproducing Figure 6 is merely an exercise in fitting.

The researchers at Bell Laboratories have carried their techniques further, enabling them to ascertain the internal charge distribution with the aid of external measurements.[3] Shown in Figure 7 is the computed charge density in Teflon for a 20 keV beam with a current density of 0.5 nA/cm^2 incident on 1 mil Teflon for 20 secs. Note the double peaked distribution of charge due to the ohmic relaxation of the initial deposited charge. Measured values of this charge density as taken from Reference 3 are shown on the same plot. It is seen that the qualitative behavior is certainly similar. Qualitatively, the calculated charge density profile is seen to be compressed in range compared to the experimental profile. Note the strong dissimilarity between this distribution and the primary deposition profile given in Reference 1.

A computation showing the evolution of the charge density to the bimodal type of distribution is shown in Figure 8 for the case of a 15 keV beam of current density of 5 mA/cm^2. The dependence of the computations on the assumed problem current density, and the assumed value of K_p is displayed in Figure 9. This figure gives the saturation charge distribution in the medium for a 15 keV beam having the indicated current density. Note the extremely strong dependence on K_p, and the essentially non-existent dependence on the current density.

IV. DISCUSSION

It may generally be said that the results presented above appear to be in agreement with experiments in a qualitative fashion, and that the quantitative agreement is approximately a factor of two. Because it might have been hoped before making this comparison that the agreement would be significantly better, some discussion of apparent sources of discrepancies is in order.

The most telling information is presented in Figure 2. The computed penetrations of the charge centroid are substantially below the measured penetrations. This suggests that either a systematic calibration error exists in the experiments or that the method of computing the primary deposition is fundamentally incorrect. We have no comment to make on the former possibility. Taking the data at face value, however, one begins to think more carefully about the primary deposition algorithm. As is evidenced on the figure, the disagreement becomes more severe for lower incident beam energies. It is well-known that the assumptions of the continuous-slowing-down-approximation[16] (CSDA) become less and less correct as the electron energy decreases. The present Monte Carlo algorithm follows the electrons to energies of 1 keV, and then deposits the electron in the final spatial bin. It might be imagined that the electrons below this energy travel somewhat further before being trapped. A test of this hypothesis requires that a non-Monte Carlo method be used for modeling the primary transport. This is possible within the state-of-the-art using the methodology developed at Oak Ridge National Laboratory for computing the differential inverse mean-free-path, and using the method of Strickland[18] to solve the resulting Boltzmann equation.

The above procedure could be used as a test of the CSDA procedure for the initial deposition profile. Note on the figure, however, that the initial location is within acceptable limits of the CSDA ranges. These discrepancies do not appear overly serious. Indeed, for a relatively low-energy beam, it is quite likely that the CSDA approximation is not sufficiently accurate. The discrepancies after the beam are on for a short time are more serious, as they show significant penetration of the beam well beyond the maximum CSDA range. This may be understood if straggling at the end of the range permits transport beyond the maximum CSDA range. Physically, this certainly happens. The abrupt drop-off in deposition which is computed with the Monte Carlo method using the CSDA leads to a significant discontinuity in the conductivity at the maximum range. The computational results are extremely sensitive to the behavior of the charge deposition and dose profiles in this region, because the internal

electric field pushes the electrons to precisely this location. It is likely that the Monte Carlo method is inadequate for handling the behavior in this region. A direct solution of the Boltzmann equation, as suggested above, should alleviate this difficulty. Should this procedure be adequate for explaining the deeper penetration of the electrons, the discrepancies shown in Figure 7 could equally well be understood. The computation is qualitatively correct, again showing significantly smaller penetration than the data.

The other major area of concern in the model is the handling of the radiation-induced conductivity (RIC) in the electron deposition region, and the transition to bulk conduction and charge transport. The behavior shown in Figure 6 cannot be explained in the present model using a conductivity which is linearly dependent on dose rate. This behavior might very well be extremely important. One can easily envision models of the discharge process in which the depth of the charge is an important parameter in determining the blow-off current. A correlation between this behavior of $\langle x \rangle$ as a function of beam current and the current density dependence of discharges which has been observed[19] might then be expected.

As explained above, the behavior shown in Figure 6 may be reproduced in the model by choosing a sublinear dependence of the RIC on dose rate. While this procedure is certainly justified based upon present understanding of RIC, it is desirable to have an independent confirmation of the parameters required to provide the data fit. This is particularly true because a recent paper by the Bell Laboratories' group[20] calls into question the simplicity of the above assumption about the proportionality of the conductivity with some power of the dose rate. Indeed, this paper suggests that the conductivity varies during the time of the irradiation. This type of behavior can be understood in terms of trap-filling in the deposition region. Requiring such an explanation, however, implies that a simple phenomenological description of the conduction process in the irradiated region is inadequate and that a more fundamental kinetic description is required. It is very likely that this situation prevails. Unfortunately, a more fundamental model will require many more fundamental parameters for its implementation. Many of these are unavailable for the materials of interest. It may be expected that the requirement for understanding low voltage discharges in spacecraft dielectrics will spawn serious attempts to quantify thermal transport processes in dielectrics.

REFERENCES

1. B. L. Beers, H. C. Hwang, D. L. Lin, and V. W. Pine, "Electron Transport Model of Dielectric Charging", in Spacecraft Charging Technology - 1978, AFGL-TR-79-0082, page 209 (1979).

2. A. R. Frederickson, "Electric Fields in Irradiated Dielectrics", Reference 1, idem., page 554.

3. G. M. Sessler, J. E. West, and D. A. Berkley, "Determination of Spatial Distribution of Charges in Thin Dielectrics", Phys. Rev. Letters 38, 368 (1977).

4. A. R. Frederickson, "Bulk Charging and Discharges Characteristics of Several Polymers", this volume.

5. B. Gross, J. E. West, H. von Seggern, and D. Berkley, "Generalized Box Model for Electron Irradiated Teflon Foils", Conference on Electrical Insulation and Dielectric Phenomena, 1980 Annual Report, page 313 (1980).

6. K. Labonte, "Charge Buildup During Electron Irradiation", Reference 5, idem., page 321.

7. N. J. Stevens, "Utilization of Charging Control Guidelines in Geosynchronous Satellite Design Studies", this volume.

8. J. J. O'Dwyer, "The Theory of Electrical Conduction and Breakdown in Solid Dielectrics", Clarendon Press, Oxford (1973).

9. M. A. Lampert and P. Mark, "Current Injection in Solids", Academic Press, New York (1970).

10. B. Gross, G. M. Sessler, and J. E. West, "Charge Dynamics for Electron-Irradiated Polymer Foil Electrets", J. Appl. Phys. 45, 2841 (1974).

11. B. Gross, G. M. Sessler, and J. E. West, "Location of Charge Centroid in Electron-Beam Charged Polymer Films", J. Appl. Phys. 48, 4303 (1977).

12. See, for example, R. E. Collins, "Use of Thermal Pulsing Technique to Obtain Information About the Distribution of Charges in Polymers", Conference on Electrical Insulation and Dielectric Phenomena, 1979 Annual Report, page 307 (1979); A. Migliorio, "A Non-Destructive Acoustic Electric Field Probe", idem., page 315; P. I. Kuindersma and R. M. van der Hey, "Dynamic Methods for the Determination of the Charge Density on Unipolar Electrets", idem., page 325.

13. E. A. Burke, J. A. Wall, and A. R. Frederickson, "Radiation-Induced Low Energy Electron Emission from Metals", IEEE Trans. Nuc. Sci., NS-19, 193 (1972).

14. J. A. Wall, E. A. Burke, and A. R. Frederickson, "Results of a Literature Search on Dielectric Properties and Electron Interaction Phenomena Related to Spacecraft Charging", in Proceedings of the Spacecraft Charging Technology Conference, C. P. Pike and R. R. Lovell, eds., AFGL-TR-77-0051, page 569 (1977).

15. R. C. Adamo, J. E. Nanevicz, and N. Grier, "Conductivity Effects in High-Voltage Spacecraft Insulating Materials", Reference 14, idem., page 669.

16. M. J. Berger, "Monte Carlo Calculation of the Penetration and Diffusion of Fast Charged Particles", in Methods in Compuational Physics, Vol. 1, Academic Press, New York (1963).

17. J. C. Ashley, "Inelastic Interactions of Low-Energy Electrons with Organic Solids: Simple Formulae for Mean Free Paths and Stopping Powers", IEEE Trans. Nuc. Sci., Vol. NS-27, No. 6, to be published.

18. D. J. Strickland and D. L. Lin, "Electron Transport Properties for Soft Electron Sources Incident on Conducting and Insulating Materials", IEEE Trans. Nuc. Sci., Vol. NS-26, No. 6, page 4879 (1979).

19. K. G. Balmain and W. Hirt, "Dielectric Surface Discharges: Dependence on Incident Electron Flux", IEEE Trans. Nuc. Sci., Vol. NS-27, to be published.

20. B. Gross, J. E. West, H. von Seggern, and D. A. Berkley, "Time-dependent Radiation-Induced Conductivity in Electron-Irradiated Teflon Foils", J. Appl. Phys. 51, page 4875 (1980).

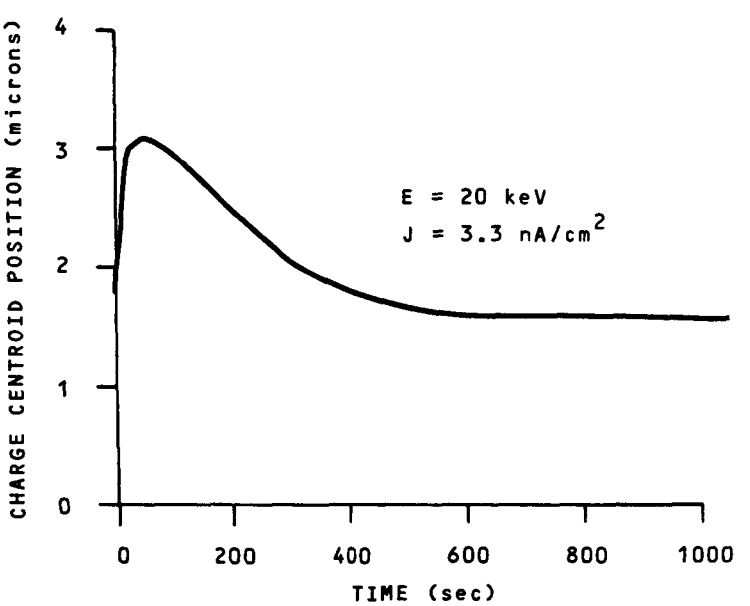

Figure 1. - Location of charge centroid as a function of time for 1 mil Teflon.

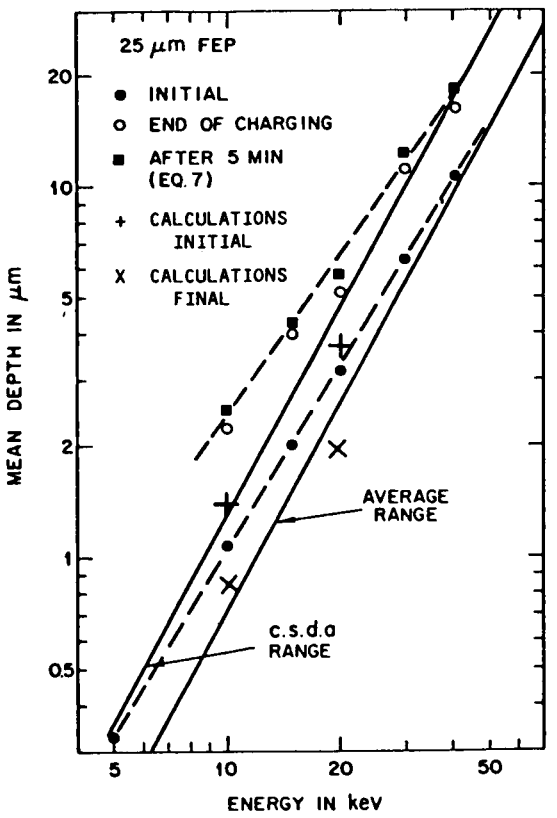

Figure 2. - Comparison of measured charge depth in Teflon with average and CSDA ranges (reproduced from ref. 11; computed results are superimposed).

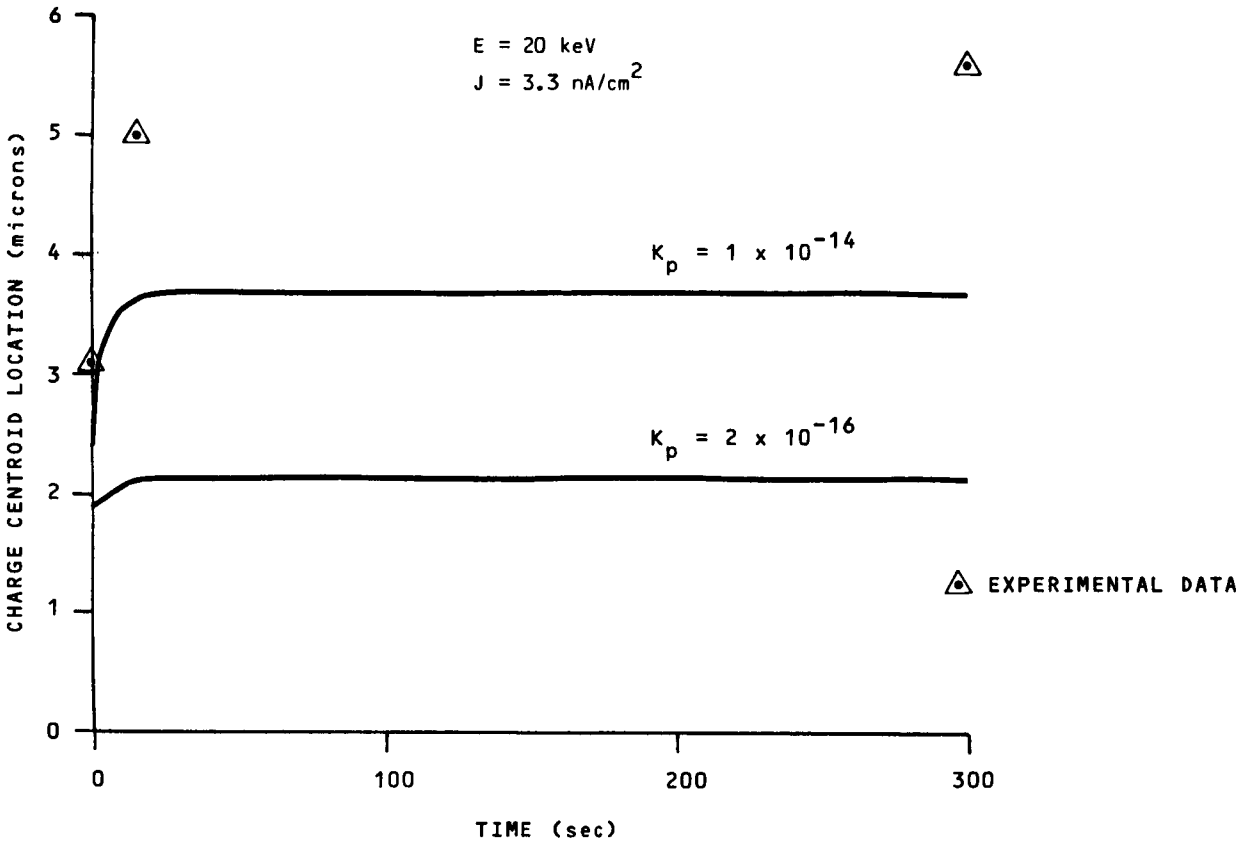

Figure 3. - Location of charge centroid as a function of time for 1 mil Teflon.

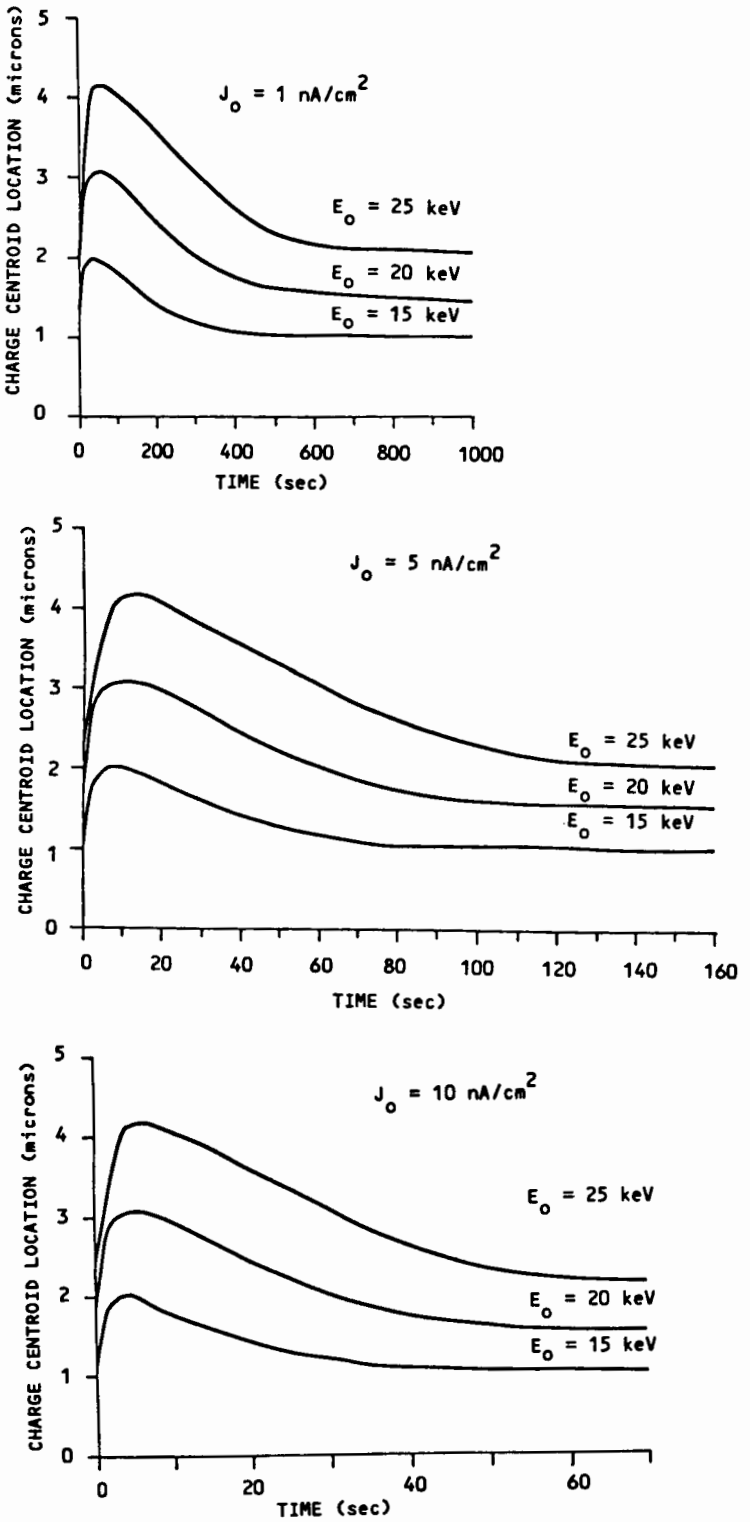

Figure 4. - Location of charge centroid as a function of time for 1 mil Teflon - various charging conditions.

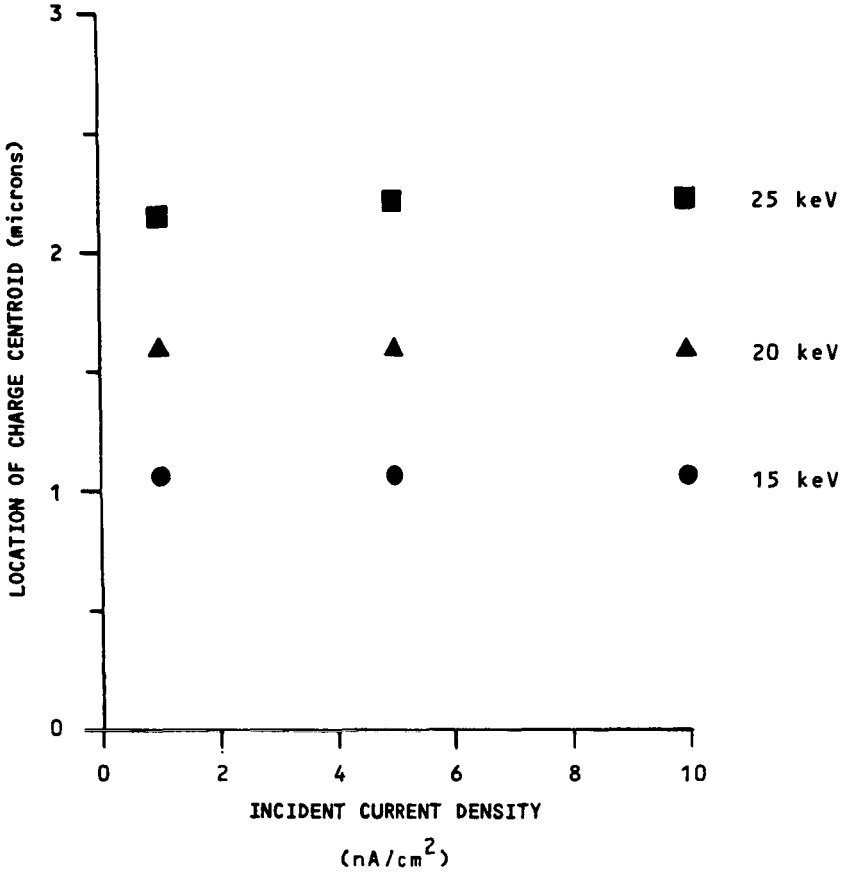

Figure 5. - Location of charge centroid for 1 mil Teflon near saturation.

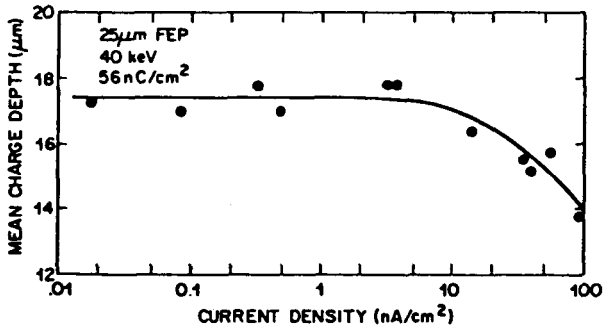

Figure 6. - Charge centroid as a function of injected current density (reproduced from ref. 11).

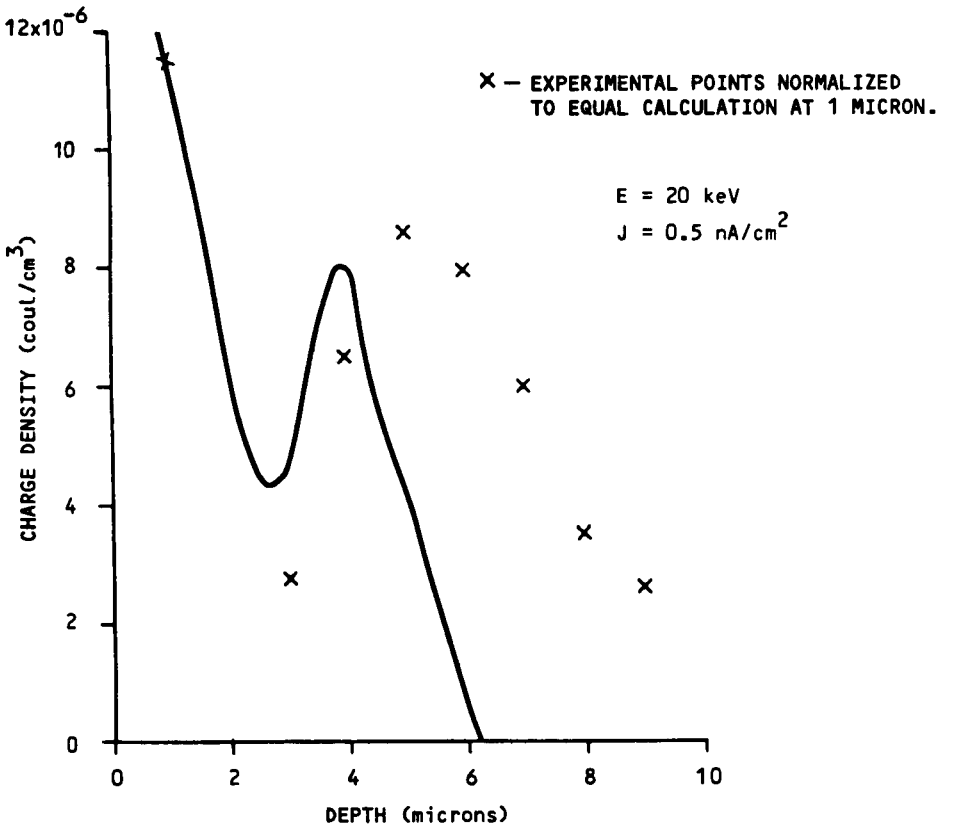

Figure 7. - Charge deposition profile for 1 mil Teflon.

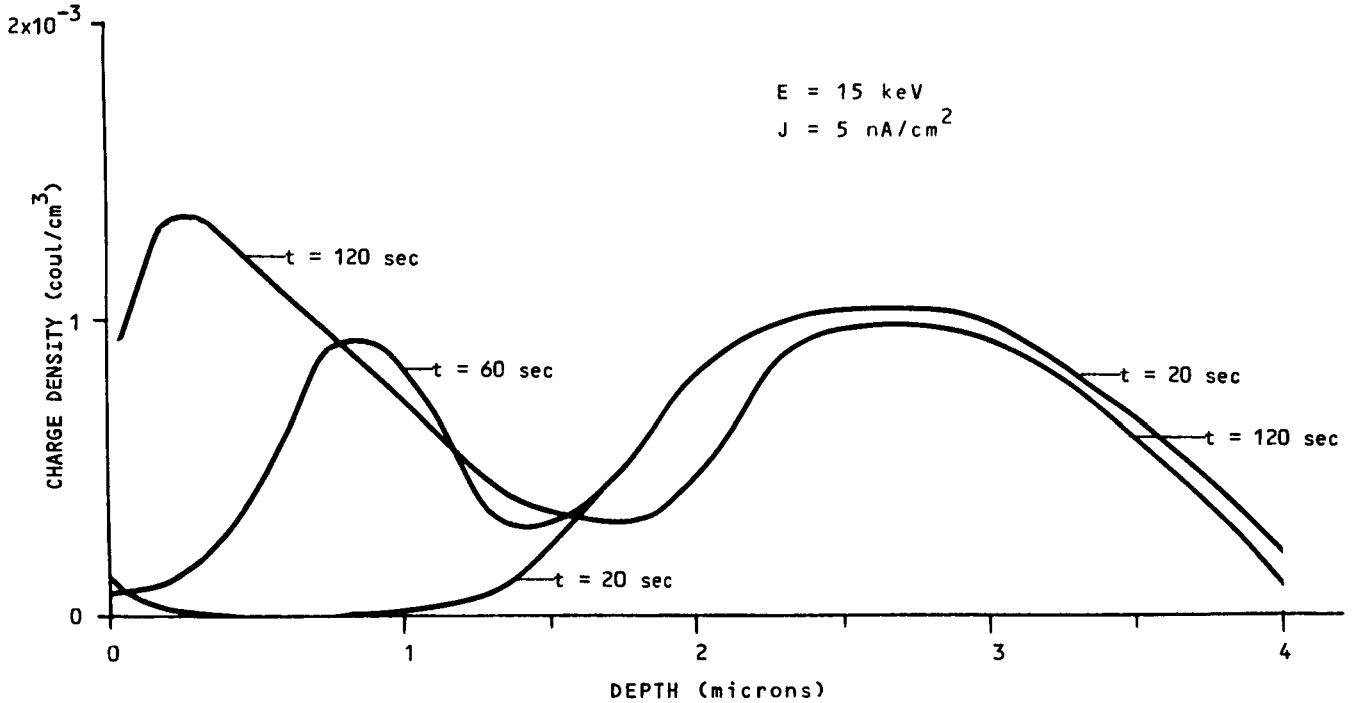

Figure 8. - Evolution of charge density of 1 mil Teflon.

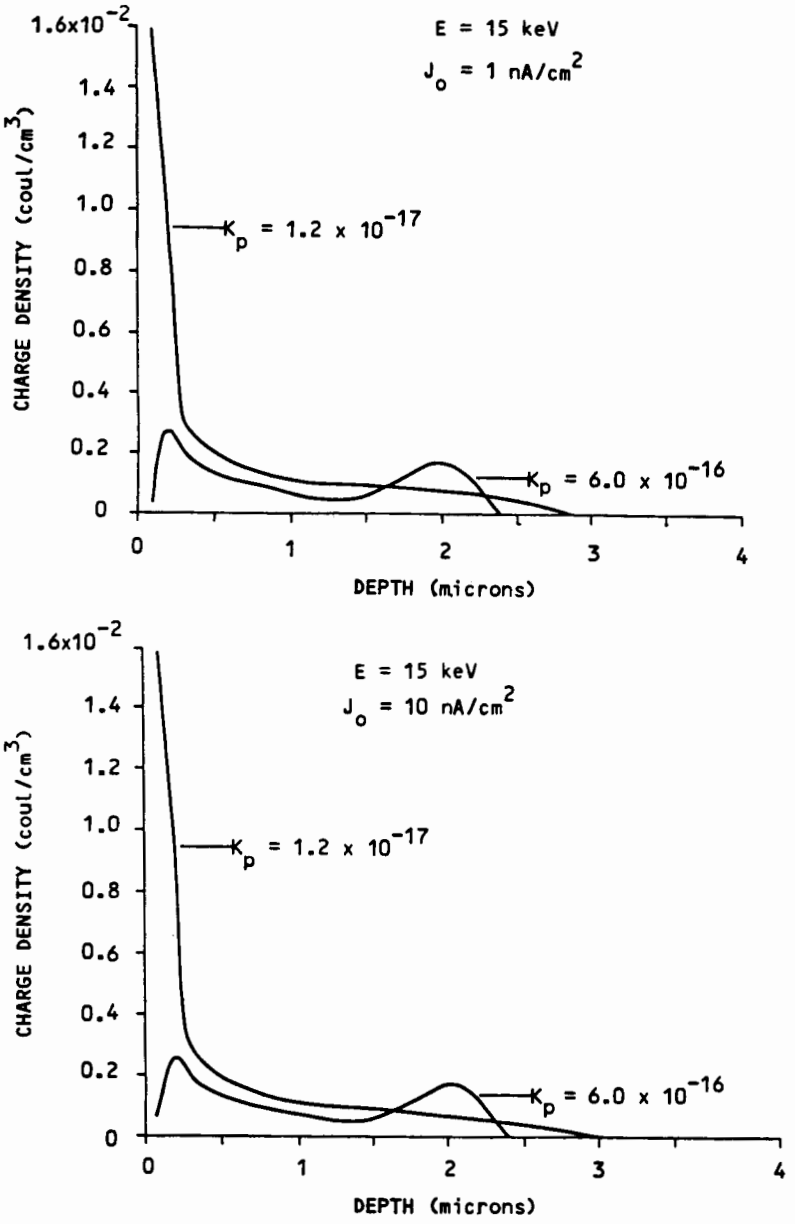

Figure 9. - Saturation ρ for various charging conditions in Teflon.